In situ Synchrotron Study of Phase Transformation Behaviors in Bulk Metallic Glass by Simultaneous Diffraction and Small Angle Scattering

X.-L. Wang,[1,2] J. Almer,[3] C. T. Liu,[2] Y. D. Wang,[1] J. K. Zhao,[1] A. D. Stoica,[1] D. R. Haeffner,[3] and W. H. Wang[4]

[1]*Spallation Neutron Source, Oak Ridge National Laboratory, Oak Ridge, Tennessee 37830, USA*
[2]*Metals and Ceramics Division, Oak Ridge National Laboratory, Oak Ridge, Tennessee 37831, USA*
[3]*Advanced Photon Source, Argonne National Laboratory, Argonne, Illinois 60439, USA*
[4]*Institute of Physics, Chinese Academy of Sciences, Beijing 100080, People's Republic of China*

(Received 30 June 2003; published 23 December 2003)

We have used a new approach involving simultaneous diffraction and small angle scattering to study the amorphous-to-crystalline phase transformation in Zr-based bulk metallic glass. *In situ*, time-resolved data provided the first direct demonstration of a phase separation prior to crystallization. There is evidence that nucleation and growth of the crystalline phase occur in separate stages, with different kinetics. Our data support the view that crystalline nucleation is achieved via short-range diffusion of small atoms (e.g., Ni), whereas the growth is dictated by long-range diffusion.

DOI: 10.1103/PhysRevLett.91.265501 PACS numbers: 61.10.–i, 61.25.Mv, 61.46.+w, 81.30.Fb

Phase transformation is a promising way for making nanostructured materials in large quantities. Bulk metallic glass (BMG) [1,2] is a case in point. Upon heating into the supercooled liquid region, BMG becomes partially crystallized resulting in a microstructure with a high density (10^{23}–10^{24} m^{-3}) of nanometer-sized crystalline particles embedded in the amorphous matrix. Nanocrystallization in BMG can be induced under a variety of conditions, including annealing, pressure treatment [3], and nanoindentation [4].

Phase transformations involving nanostructured materials usually occur under conditions far from equilibrium. Although thermodynamics ultimately determines the equilibrium phase for a given set of conditions, whether and how the nanostructured phase is produced from the metastable precursor depends on kinetic processes. Our current knowledge of phase transformations in BMG was mostly built upon *ex situ* experimental work [5–14] on samples that had undergone such transformations. Only a few *in situ* studies [15–17] have been reported, which begin to provide details of the transformation behaviors at elevated temperatures. The lack of *in situ*, time-resolved data in the early stage of crystallization leaves many unresolved questions. In particular, the mechanisms of nucleation remain a subject of debate [2,9,12,14,15,18–21]. Classical nucleation theory cannot give rise to such a high density of crystalline particles at temperatures close to the glass transition temperature [18], because the kinetics is too slow. Heterogeneous nucleation on impurity sites [19,20] has been considered. Indeed, there is evidence that the crystalline phase in $Zr_{52.5}Cu_{17.9}Ni_{14.6}Al_{10}Ti_5$ containing oxygen impurities grows out of the tiny Zr_4Ni_2O [20] nucleus. However, the density of these impurity sites is usually orders of magnitude lower than that of the nanocrystalline particles in partially crystallized BMG. Phase separation [2,12,21] has been proposed as another possibility in which the BMG decomposes into two or more amorphous phases before the onset of an amorphous-to-crystalline transformation. Previous small angle neutron scattering studies on a number of BMG systems [12–15], most notably $Zr_{41.2}Ti_{13.8}Cu_{12.5}Ni_{10}Be_{22.5}$, revealed scattering profiles reminiscent of phase separation behaviors found in crystalline metallic alloys [22]. However, small angle scattering (SAS) data alone cannot tell when the crystalline phases are forming. Obviously, without a direct experimental demonstration, the argument for nucleation through phase separation is difficult to sustain. In fact, a recent investigation [9] of partially crystallized $Zr_{57}Cu_{20}Ni_8Al_{10}Ti_5$, combining differential scanning calorimetry (DSC), x-ray diffraction (XRD), and transmission electron microscopy (TEM), suggests just the opposite. In this Letter, we report an *in situ* synchrotron study involving simultaneous measurements of diffraction and SAS data, which provided direct evidence of a phase separation prior to crystallization.

The BMG used in our synchrotron experiment was BAM-11, with the composition $Zr_{52.5}Cu_{17.9}Ni_{14.6}Al_{10}Ti_5$ [7,8]. The samples were 1 mm thick disks with a diameter of 8 mm. The glass and crystallization temperatures, T_g and T_x, were 628 K and 714 K, respectively, determined from DSC at a heating rate of 10 K/min. Annealing at 681–713 K leads to 2–10 nm crystalline particles based on XRD and TEM studies.

Our *in situ* annealing study was carried out at the 1-ID beam line of the Advanced Photon Source at Argonne National Laboratory, using 77 keV x rays. Thick samples can be measured in transmission with high-energy x rays, ensuring that the probing volume ($0.1 \times 0.1 \times 1$ mm^3 in our case) was representative of the bulk of the material. 1-ID has been primarily used for *in situ* diffraction studies [23], but recently small angle x-ray scattering (SAXS) experiments were successfully demonstrated [24] with a Q range of 0.008–0.2 $Å^{-1}$, where Q is the magnitude of the momentum transfer. In order to determine the kinetics of both phase separation and crystallization, we

have modified the instrument to record simultaneously the diffraction and SAS intensities using two area detectors. To our knowledge, this is the first time that simultaneous diffraction and SAS measurements are made with high-energy x rays.

Figure 1(b) shows the kinetic diagram of the diffraction patterns in the early stage of phase transformation. A remarkable feature is the abrupt change at $t = 40$ min, when diffraction peaks suddenly appeared and the amorphous background began to recede [Fig. 1(c)]. The crystalline phase was identified to be primarily tetragonal Zr_2Ni, consistent with previous studies [8]. In a repeat experiment (with a different sample), partial transformation to a second crystalline phase was observed upon continuing heating to higher temperatures.

Figure 1(d) shows the kinetic diagram of the SAS profiles. Scattering at room temperature has been subtracted so the data shown here represent the formation and growth of a new phase. The scattering profiles are characterized by an interference peak at $Q_{\max} \sim 0.02$–0.03 Å^{-1}, which decreases with increasing annealing times [Fig. 1(e)]. Guinier analysis over the Q range 0.032–0.050 Å^{-1} yields a representative particle size, D_g, of about 15.0 ± 0.3 nm in final equilibrium.

With the diffraction and SAS data measured simultaneously, we are now able to uncover how the BMG material transforms by exploring the kinetics at two different length scales. A close examination of Fig. 1(d) shows that SAS intensity began to develop at $t = 36$ min, well before the onset of crystallization, which occurred at $t = 40$ min as revealed by the diffraction data. To further illustrate this point, we plot in Fig. 2(a) the integrated intensities from diffraction and SAS as a function of time. The diffraction intensity was calculated as follows: $I_D = |Y(t, Q) - Y(t_0, Q)|$, where $Y(t, Q)$ is the x-ray intensity at Q for a given data set collected at time t and t_0 is a time prior to the transformation. For the cluster of peaks centered around $d = 1.0$ Å, the amorphous background is essentially flat, so that $I_D \propto VF^2$, where V is the volume and F is the structure factor of the crystalline phase. The above relationship is generally true so long as the scattering function from the amorphous matrix does not change appreciably during crystallization. A comparison of the I_D values calculated for each of the three

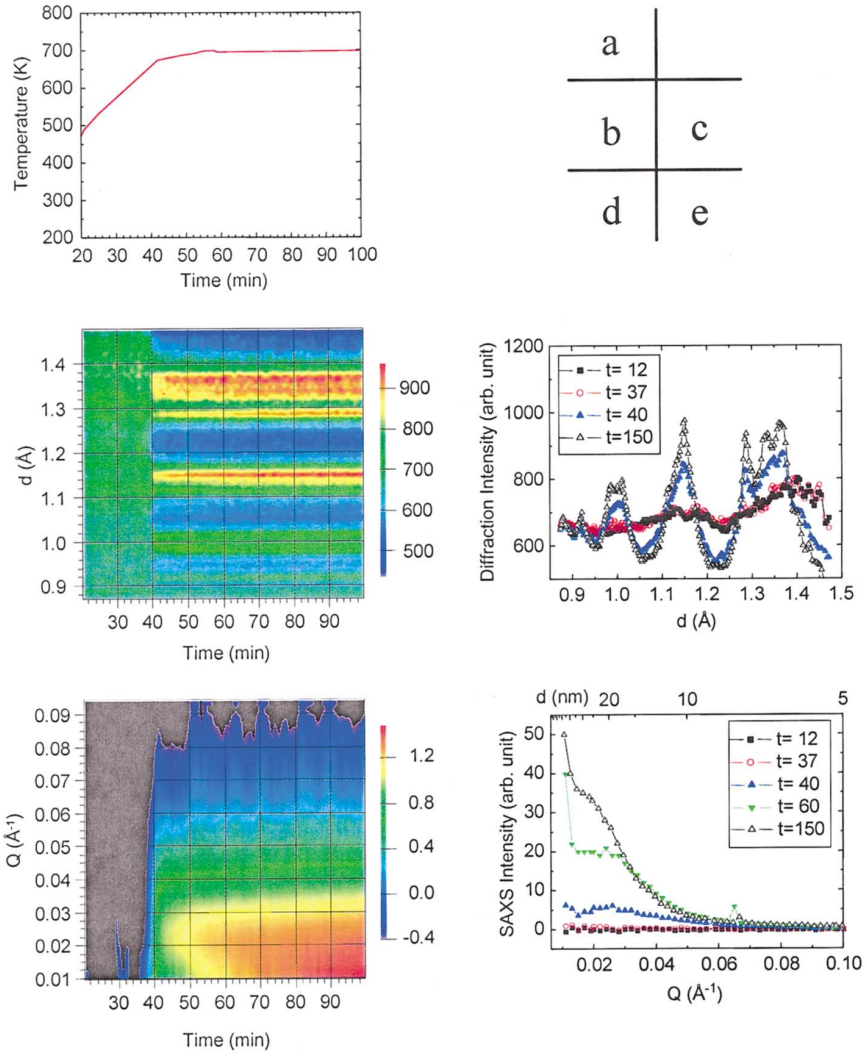

FIG. 1 (color). Simultaneous diffraction and SAXS data obtained with high-energy ($E = 77$ keV) synchrotron x ray. The sample was heated in vacuum at a heating rate of approximately 10 K/min, reaching the equilibrium temperature of $T = 696$ K at $t = 53$ min. The experimental data were recorded every minute, with an exposure time of 0.5 min, throughout the annealing experiment. (a) Temperature of the sample for $20 < t < 100$ min. (b) Kinetic diffraction diagram for $20 < t < 100$ min. (c) Diffraction patterns at selected annealing times. Prominent diffraction peaks appeared at $t = 40$ min. (d) Kinetic diagram of SAXS intensity for $20 < t < 100$ min (in log scale). (e) SAXS profiles at selected annealing times. The top axis gives the corresponding length scale ($d = \frac{2\pi}{Q}$) that is being probed.

clusters of peaks showed consistent time dependence. The calculated I_D values were therefore added and the sum is plotted in Fig. 2(a). The SAS intensity, I_S, is a sum over the Q range of 0.01–0.10 Å^{-1}. The inset of Fig. 2(a) highlights the evolution of I_D and I_S from $t = 30$ to $t = 46$ min. It is clear that the phase separation began to develop as early as $t = 36$ min. By contrast, a sharp amorphous-to-crystalline phase transformation occurred at $t = 40$ min.

Our data provided direct evidence of a phase separation prior to crystallization. Furthermore, the experiment data show that partial crystallization in $Zr_{52.5}Cu_{17.9}Ni_{14.6}Al_{10}Ti_5$ BMG proceeds in two separate stages, nucleation and growth, with distinctively different kinetics. The solid line through I_D in Fig. 2(a) is a fit using the John-Mehl-Avrami (JMA) transformation theory, which estimates the volume fraction of transformed materials as $x(t) = 1 - \exp\langle -k(t - t_0)^n \rangle$. The fit yielded an exponent $n = 0.33 \pm 0.03$. In classical theory of diffusion-controlled transformation, the exponent n is often used to characterize the mechanisms of transformation [25]. At short times n varies between 1 and 2.5; the lower limit corresponds to diffusional growth of embedded nuclei by boundary diffusion whereas the upper limit corresponds to bulk growth of precipitates nucleating during crystallization [10]. The value of n decreases to 0.5 when diffusion zones start to overlap (soft impingement) and the crystallization rate is slowed down (see below). Thus, the value of $n = 0.33$ obtained for I_D indicates that the diffusion zones are overlapping. This is not surprising in view of the large number ($\sim 10^{23}$–10^{24} m^{-3}) of nanosized precipitates that developed. The parameter $k = 0.26 \pm 0.03$, corresponding to a relaxation time of $\tau_D = 1.6$ min.

The excellent fit with the JMA equation indicates that the dominant feature for $t > 40$ min is the growth of the volume fraction due to long-range diffusion. This observation is further corroborated by analysis of the SAS data. If we consider partially crystallized BMG consisting of uniform-sized crystalline particles in a glass matrix, $I_D \propto V = Nv$, where N and v are, respectively, the number and average volume of the crystalline particles. v is related to the Guinier particle size D_g obtained from SAS, $v \sim D_g^3$. As shown in Fig. 2(b), a nearly linear relationship exists between I_D and D_g^3 for $t > 40$ min. This means that the increase of I_D and I_S is primarily due to the growth of the particle volume, v, rather than the number of particles, N. A corollary is that nucleation of the crystalline particles is completed before $t = 40$ min or the onset of crystallization.

The slow growth kinetics indicated by the evolution of I_D is a consequence of the strong liquid behavior typically found in BMG. Previous studies [5,6,26,27] have established that the viscosity of BMG in the supercooled liquid region follows the Vogel-Fulcher-Tammann (VFT) relationship, with a fragility parameter [28] that is an order of magnitude larger than typical fragile liquids. The strong liquid behavior resulting from increased viscosity leads to lower atomic mobility. Quasielastic neutron scattering studies [29] have demonstrated that the long-range diffusivity in liquid $Pd_{40}Ni_{10}Cu_{30}P_{20}$ is on the order of 10^{-10} m^2 s^{-1}, some 3 orders of magnitude slower than in simple metallic liquid.

The evolution of the SAS intensity for $t < 40$ min characterizes the nucleation stage of the crystalline phase. In the inset of Fig. 2(a), the solid line through I_S is a fit with exponential growth, which describes very well the evolution of I_S up to $t = 40$ min when an abrupt crystallization occurred. The fitted parameter τ_S is 1.4 ± 0.1 min. The growth of I_S is disrupted at the onset of crystallization.

Long-range atomic diffusion, which is responsible for the slow growth kinetics seen in I_D, cannot account for the rapid exponential increase of I_S during nucleation ($t < 40$ min). Instead, short-range atomic transport

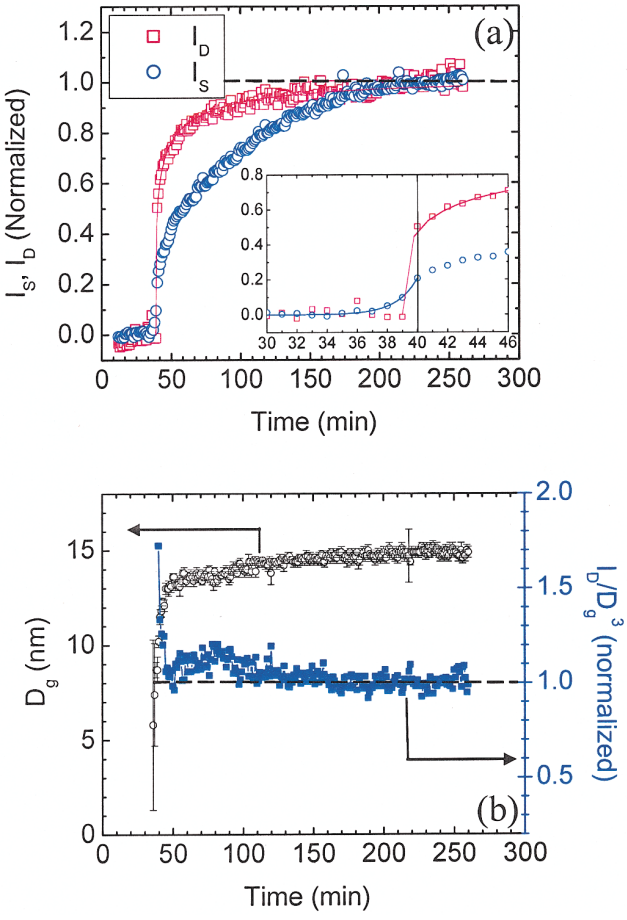

FIG. 2 (color). (a) Integrated diffraction I_D and small angle scattering I_S intensities as a function of time. (b) Evolution of D_g and $\frac{I_D}{D_g^3}$. D_g is a representative particle size determined from a Guinier analysis of the SAS data. For a system consisting of uniform-sized particles, $\frac{I_D}{D_g^3} \propto N$, where N is the number of particles. The flat profile seen for $\frac{I_D}{D_g^3}$ indicates that N is held constant during growth. The values of I_D, I_S, and $\frac{I_D}{D_g^3}$ have been normalized to unity (dashed lines) at equilibrium ($t > 200$ min).

must be considered. It is important to recognize that atomic diffusion in BMG proceeds via two parallel processes, single-atom hopping and collective motions of groups of atoms [5,26]. The former dominates below T_g whereas the latter dominates above T_g [26]. In $Zr_{52.5}Cu_{17.9}Ni_{14.6}Al_{10}Ti_5$, previous [8] and present studies show that the crystalline phase obtained by annealing at $T \sim 700$ K is primarily Zr_2Ni, suggesting that Ni and/or Zr atoms are involved in nucleation. However, tracer-diffusion measurements in several BMG materials [6,27] have consistently demonstrated that large atoms such as Zr and Al are slow, with diffusion constants that are orders of magnitude smaller than that of Ni. By contrast, Ni atoms remain mobile even at temperatures slightly below T_g [6], where the viscosity increased by several orders of magnitude. Thus, a possible scenario for nucleation of the crystalline phase is the homogenous formation of Ni-rich clusters due to local exchange of atoms. Such a mechanism is energetically favored, as pointed out by Egami [30] who considered local topological instability generated by supercooling. Separately, Tanaka [31] argued that in strong glass formers, there is a strong tendency of short-range bond ordering in the supercooled liquid state. Thus, the formation of Ni-rich clusters is both energetically possible and kinetically allowed. Indeed, in our experiment, the first appearance of the SAS intensity was captured during heating at $T = 630$ K, just above T_g.

The proposed mechanism provides an adequate qualitative account for our experimental observations. For a multicomponent BMG with a composition close to deep eutectic, a large number of clusters can form as a result of local atoms exchange enabled by short-range diffusion of the mobile atoms (e.g., Ni). This is a fast, interface-controlled process involving only neighboring atoms. The formation of Ni-rich clusters also creates depleted diffusion zones which overlap due to the high density of clusters, as indicated by the fitted exponent of $n = 0.33 \pm 0.03$ for I_D. The overlap of the clusters generates a complex composition modulation similar to that involved in spinodal decomposition [32], which explains very well the interference peaks observed in SAS profiles [14,22] and the exponential growth of I_S. Continued phase separation moves the composition of the subcritical particles closer to that of the developing crystalline (Zr_2Ni) phase, which eventually triggered the amorphous-to-crystalline phase transformation.

The development of a diffusion zone also affects the transformation. Assadi and Schroers showed [18], using the Ginzberg-Landau theory, that a diffusive layer could lower the activation energy barrier for crystallization and at sufficient thickness, the activation energy barrier disappears entirely, creating a cascade type of transition as indicated by our diffraction data. This is also the moment when the increase of I_S slows down because the neighboring supply of Ni is depleted. Further growth of the diffraction and SAS intensities then has to come from the long-range diffusion dictated by the strong liquid behavior of the material.

In summary, a new approach involving simultaneous measurements of diffraction and SAS data allowed us to probe the kinetics of phase transformations at different length scales. Our experiment shows that nucleation and growth of the crystalline phase in $Zr_{52.5}Cu_{17.9}Ni_{14.6}Al_{10}Ti_5$ BMG occur in separate stages, with different kinetics. Phase separation occurred first, setting the stage for crystallization. A mechanism based on short-range atomic transport is proposed for phase separation.

This research was supported by Division of Materials Sciences and Engineering, Office of Basic Energy Sciences, U.S. Department of Energy under Contract No. DE-AC05-00OR22725 with UT-Battelle, LLC.

[1] W. L. Johnson, MRS Bull. **24**, No. 10, 42 (1999).
[2] A. Inoue, Acta Mater. **48**, 279 (2000).
[3] W. H. Wang *et al.*, Appl. Phys. Lett. **75**, 2770 (1999).
[4] J.-J. Kim *et al.*, Science **295**, 654 (2002).
[5] A. Masuhr *et al.*, Phys. Rev. Lett. **82**, 2290 (1999).
[6] R. Busch, J. Met. **52**, No. 7, 39 (2000).
[7] J. G. Wang *et al.*, J. Mater. Res. **15**, 798 (2000).
[8] T. G. Nieh *et al.*, Mater. Trans. JIM **42**, 613 (2001).
[9] A. Revesz *et al.*, Philos. Mag. Lett. **81**, 767 (2001).
[10] A. S. Bakai, H. Hermann, and N. P. Lazarev, Philos. Mag. A **82**, 1521 (2002).
[11] A. T. W. Kempen, F. Sommer, and E. J. Mittemeijer, Acta Mater. **50**, 1319 (2002).
[12] S. Schneider, P. Thiyagarajan, and W. L. Johnson, Appl. Phys. Lett. **68**, 493 (1996).
[13] H. Hermann, A. Weidenman, and P. Uebele, Physica (Amsterdam) **241B–243B**, 352 (1998).
[14] H. Hermann *et al.*, J. Appl. Crystallogr. **34**, 666 (2001).
[15] J. F. Löffler *et al.*, Appl. Phys. Lett. **77**, 525 (2000).
[16] N. Mattern *et al.*, Appl. Phys. Lett. **80**, 4525 (2002).
[17] K. F. Kelton *et al.*, Phys. Rev. Lett. **90**, 195504 (2003).
[18] H. Assadi and J. Schroers, Acta Mater. **50**, 89 (2002).
[19] T. Ohkubo *et al.*, Scr. Mater. **44**, 971 (2001).
[20] C. T. Liu, M. F. Chisholm, and M. K. Miller, Intermetallics **10**, 1105 (2002).
[21] J. F. Löffler and W. L. Johnson, Appl. Phys. Lett. **76**, 3394 (2000).
[22] P. Fratzl, J. Appl. Crystallogr. **36**, 397 (2003).
[23] Y. D. Wang *et al.*, J. Appl. Crystallogr. **35**, 684 (2002).
[24] A. Kulkarni *et al.*, J. Am. Ceram. Soc. (to be published).
[25] R. D. Doherty, in *Physical Metallurgy*, edited by R. W. Cahn and P. Haasen (Elsevier Science B.V., North-Holland, Amsterdam, 1996), pp. 1364–1505.
[26] X.-P. Tang *et al.*, Nature (London) **402**, 160 (1999).
[27] F. Faupel *et al.*, Rev. Mod. Phys. **75**, 237 (2003).
[28] C. A. Angell, Science **267**, 1924 (1995).
[29] A. Meyer, R. Busch, and H. Schober, Phys. Rev. Lett. **83**, 5027 (1999).
[30] T. Egami, Z. Metallkd. **93**, 1071 (2002).
[31] H. Tanaka, Phys. Rev. Lett. **90**, 055701 (2003).
[32] J. W. Cahn, J. Chem. Phys. **42**, 93 (1965).